Azimuthal Structure and Global Instability in the Implosion Phase of Wire Array *Z*-Pinch Experiments

S. V. Lebedev, I. H. Mitchell, R. Aliaga-Rossel, S. N. Bland, J. P. Chittenden, A. E. Dangor, and M. G. Haines
Imperial College, Blackett Laboratory, Prince Consort Road, London SW7 2BZ, United Kingdom
(Received 30 June 1998)

The implosion of aluminum wire array z pinches driven by a 1.4 MA, 240 ns current pulse is studied. Plasma evolution is measured in the r-θ plane for the first time by an end-on laser interferometer. Merging of coronal plasmas with density of 10^{17} cm^{-3} occurs in 90–65 ns for 16 mm diam arrays with 8–64 wires. Early uncorrelated instabilities (wavelength $\lambda \sim 0.5$ mm) are observed in individual wires with later development of a global $m = 0$ instability ($\lambda \sim 2$ mm). The number of Rayleigh-Taylor instability e foldings is 5.6–7 when the $m = 0$ instability reaches an observable level and increases with the number of wires. [S0031-9007(98)07542-5]

PACS numbers: 52.55.Ez

Fast z-pinch implosions are an effective way of converting stored electrical energy into x rays. Among other applications [1], pinch x-ray sources are used to energize hohlraums to blackbody temperatures of ~150 eV [2] for experiments relevant to indirect drive inertial confinement fusion. Power levels up to ~200 TW [3] have been obtained using cylindrical arrays with large numbers (~240) of thin metallic wires as a z-pinch load. There is a general understanding that the high degree of symmetry of the load in large wire number shots is a key factor in attaining high x-ray power [4]. Assuming the plasma from the wires forms a uniform shell, two dimensional (r-z) magnetohydrodynamic (MHD) modeling [4,5] can reproduce the observed x-ray pulse width by adjusting the level of seeded perturbations, from which the magnetic Rayleigh-Taylor (RT) instability grows. The required level of these perturbations is smaller for arrays with larger number of wires. Despite the importance of initial plasma formation, the experimental database has concentrated upon measurements of x-ray characteristics at stagnation and the final part of implosion. Furthermore, there is no direct experimental evidence of shell formation. Indeed, early experiments [6] with a small number of wires and large interwire separation show radial streams of plasma from wires, which fill the interior of the array with plasma. Even for a large number of wires (120) and small interwire spacing (0.46 mm) [7], no uniform shell was formed during the observation time, the first 60% of the implosion time.

In this Letter we report on measurements of the dynamics of plasma formation in wire array z pinches. The azimuthal structure of the plasma inside the array and merging of the coronal plasmas from adjacent wires was measured by end-on laser probing. Prior to this, side-on probing has shown that plasma expansion from individual wires occurs with development of the MHD "sausage" instability, driven by the private magnetic field of each wire but modified by the global magnetic field of the array. At later time a global $m = 0$ instability with a dominant wavelength of 1.7–2.3 mm was detected. The time when the instability becomes observable corresponds to the number of e foldings for the growth rate of the classical RT instability of $\int \gamma\, dt \sim 5.6$–7. This number increases with the number of wires in the array according to $\exp(\int \gamma\, dt) \propto N^{1/2}$. Such a dependence is to be expected if the instability grows from a level of initial perturbations determined by the averaging of uncorrelated density perturbations in individual wires [8].

Experiments were performed on the MAGPIE generator [9] with a current rising to 1.4 MA in 240 ns (10% to 90% rise time is 150 ns). Wire arrays 16 mm in diameter and 2.3 cm long with 8, 16, 32, and 64 aluminum wires of 15 μm diameter provided stagnation near the current maximum and a dense hot plasma was formed on axis. The experimental arrangement allowed the use of both end-on (r-θ plane) and side-on (r-z plane) laser probing (Nd-YAG, 532 nm, 0.4 ns) giving interferometry, schlieren, or shadow images. Time-resolved soft x-ray images were obtained with a gated 4-frame camera (2 ns gate time with 9 ns separation).

Figure 1 shows a set of end-on (r-θ plane) interferograms obtained for arrays of 8 and 16 wires. A fringe shift of one fringe corresponds to an electron density of 9×10^{16} cm^{-3} for the probing path along the pinch axis of 2×2.3 cm. At times less than 60 ns ($t = 0$ is the current start), the plasma density inside the array is below the sensitivity of the interferometer ($n_e < 3 \times 10^{16}$ cm^{-3}). After this the plasma starts to move inside the array in the form of radially directed streams. The plasma formed around the initial wire positions has the highest density and here the probing laser beam is deflected out of the optical system. Outside these regions the plasma density gradients are lower and a shift of interference fringes, corresponding to electron density in the range (3×10^{16})–(5×10^{17}) cm^{-3}, can be measured. The line density of electrons inside arrays with 8 wires obtained by integrating the density distribution is $\sim 5 \times 10^{17}$ cm^{-1} at 90 ns after the current start, which gives an upper limit estimate of the mass of 60% of the total load mass, if it is

 0031-9007/98/81(19)/4152(4)$15.00

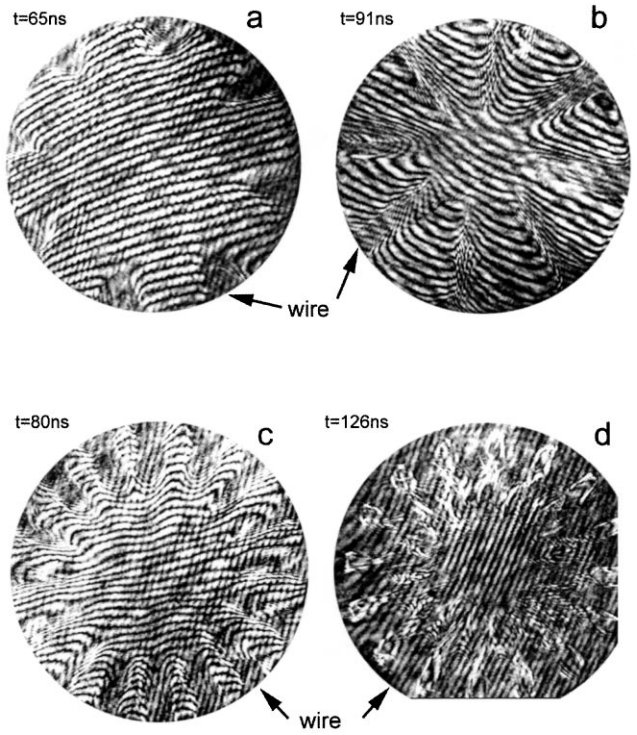

FIG. 1. End-on (r-θ plane) interferograms of arrays with 8 (a),(b) and 16 (c),(d) wires showing radial plasma jets from the wires. Vertical fringes in the center of image (d) are an artifact of the reference laser beam.

singly ionized. However, two-dimensional resistive MHD simulations of single Al wire pinches, similar to those published for carbon pinches [10], indicate that regions of the corona with electron density comparable to the sensitivity of the interferometer are of high temperature ($\sim$30 eV) and have an ion charge of $\sim$10. This decreases the previous mass estimate to 5%. In our experiment, the plasma electron density contour of 10^{17} cm^{-3} has an inward radial velocity of 15 cm/μs. From the shape of the density contours, it can be seen that the azimuthal velocity is 1/4 of radial velocity. Azimuthal expansion leads to merging of the coronal plasmas, and plasma with density $>10^{17}$ cm^{-3} fills regions between the wires at the initial radius of the array at 65 and 90 ns for arrays with 64 and 8 wires (gap size 0.78–6.28 mm), respectively. Merging also results in the formation of plasma with an even higher density at this time in some regions within the array. End-on images, obtained later in the discharge [Fig. 1(d)], show that the density gradients inside the array are almost everywhere too high to allow the probing laser beam to pass through the plasma. Only in the regions between the initial wire positions is the density of plasma lower and consequently interference fringes are visible. This observation suggests that the density distribution is highly nonuniform in the azimuthal direction even after merging of the coronal plasmas.

Side-on laser probing (Fig. 2) shows that the coronal plasma of individual wires expands with the development

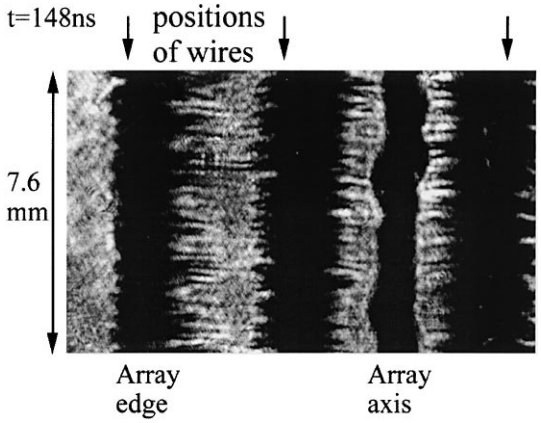

FIG. 2. Side-on schlieren (r-z plane) of array with 8 wires showing coronal plasma (dark areas) around the wires and the precursor on the array axis.

of instabilities with an axial wavelength of less than 0.5 mm. Comparison of the instabilities in different wires shows that they are not correlated during the initial stage of the discharge. These instabilities are similar to those formed in single wire z pinches [11–13], but the presence of the global magnetic field of the array modifies the instability pattern, which is no longer symmetric around the wire axis. Expansion rates of the coronal plasma in the radial and azimuthal directions are shown in Fig. 3. The sensitivity of the schlieren system used for these measurements corresponds to a line integral of the orthogonal gradient of electron density of 1.5×10^{19} cm^{-3}. The coronal plasma expands at a speed of 3.2 ± 0.3 cm/μs in the inward radial direction and at 1.3 ± 0.1 cm/μs in the azimuthal direction beginning at $\sim$60 ns when the total current is 250 kA. Before this time only a slow expansion of the plasma is observed at a speed of $\sim$0.2 cm/μs, which is close to the thermal velocity of Al atoms at boiling temperature. Expansion of the wires radially outwards is always at the slow speed of $\sim$0.2 cm/μs (Fig. 3). Note that the delay in the start of the faster expansion of the coronal plasma of $\sim$60 ns is the same in side-on and end-on probing. The

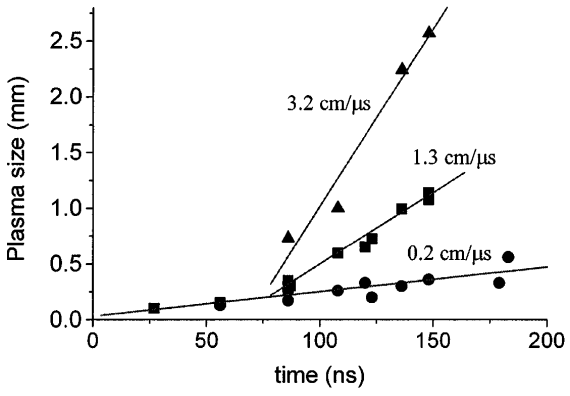

FIG. 3. Coronal plasma size in azimuthal (■) and radial [(▲) inward, (●) outward] directions as a function of time.

velocities are different, however, which can be explained by the different densities measured in each diagnostic ($n_e \sim 1.5 \times 10^{19}$ cm^{-3} side-on and 10^{17} cm^{-3} end-on).

The coronal plasma accelerated radially inwards from the wires by the pressure of the global magnetic field arrives on axis before the array implosion, where it accumulates to form the precursor plasma. Precursor plasma was detected in early experiments [6,14] with a small number of wires ($\sim$10). In the experiments reported here, this plasma forms a uniform narrow and relatively stable column of diameter $\sim$1 mm as measured from radial optical streak photographs, x-ray gated images, and laser probing (Fig. 2). Precursor formation occurs at $\sim$120 ns for all numbers of wires used and agrees well with the inward velocity of 15 cm/μs of the low density coronal plasma found from end-on measurements. However, the intensity and diameter of precursor plasma emission in both the optical and the x-ray regions decrease as the number of wires in the array increases. Results of detailed measurements of the precursor will be published separately.

During the later stages of array implosion, the development of an $m = 0$ instability in the global magnetic field was observed by several diagnostics, starting at time $t/t_{\text{imp}} \sim 0.7$–$0.8$ (where t_{imp} is the calculated time of implosion). At this time x-ray gated images, filtered to transmit L-shell lines of Al (5 μm polycarbonate, transmission window between 100 and 190 eV), show nonuniform emission from the wires, and a number of bright spots are formed at the initial radial positions of wires (Fig. 4). These bright spots are formed on all wires and their axial positions are correlated between different wires. The axial spatial separation between spots averaged over the length of the wire varies slightly with the number of wires and is between 1.7 and 2.3 mm. The time of spot formation depends on the number of wires, as shown in Table I. Bright spots are formed in a time comparable with the interframe time (9 ns) of the camera [compare images in Fig. 4(a)] and emission from the bright spots lasts almost until stagnation time. During all this time the bright spots do not change their radial positions which, for small numbers of wires (8 and 16), exactly coincide with the initial wire positions. For arrays with 64 wires, an inward radial displacement of bright spots from the edge wire position of only 1 mm (array radius 8 mm) was measured at the time of their formation $t/t_{\text{imp}} = 0.87$. This is in great contrast both with the calculated position of a thin imploding shell of the same mass per unit length and with the position of the inner boundary of the imploding plasma as measured from radial optical streak photographs, which both give $r/r_0 \sim 0.5$. However, the total implosion time measured from radial streak photographs is in good agreement with the calculated times for both 64 and smaller numbers of wires.

This behavior is consistent with the presence of a nonionized dense core in the wires, similar to that observed in experiments with single Al wires [12], which does not carry sufficient current to be accelerated by the $\mathbf{J} \times \mathbf{B}$ force. Development of the instability may lead to a more rapid ionization of the core, which will be nonuniform in the z direction, and also to a subsequent nonuniform implosion of the array. The same characteristic wavelength of $\sim$2 mm at the time of instability development is also seen in side-on laser probing images, which show formation of radial plasma streams and gaps (Fig. 5). Orientation of the array relative to the laser beam is such that each arrow in Fig. 5 indicates the position of two wires of the array, one behind the other. Consequently, the gaps observed must be correlated in at least two wires.

The development of this global instability is consistent with the merging of the coronal plasmas from the individual wires which was observed by the end-on interferometry earlier in the discharge. The strongest candidate for the instability is the Rayleigh-Taylor instability in a plasma accelerated by the magnetic pressure. It is well established [15] that for imploding z pinches the RT instability is a limiting factor in achieving high energy density and power of x-ray pulse. A number of 2D (r-z) MHD computer models have been developed to describe the dynamics of z-pinch implosions [5,16,17]. These models accurately reproduce the shape of the x-ray pulse at stagnation observed in experiments by employing *ad hoc* assumptions of the RT seed level. To reach agreement with data from experiments with different number of wires in the array, levels of random density perturbation between 30% (small number of wires $N \sim 20$) and 5% ($N \sim 100$) are required [4,18]. For the classical RT instability, seeded perturbations will grow linearly as

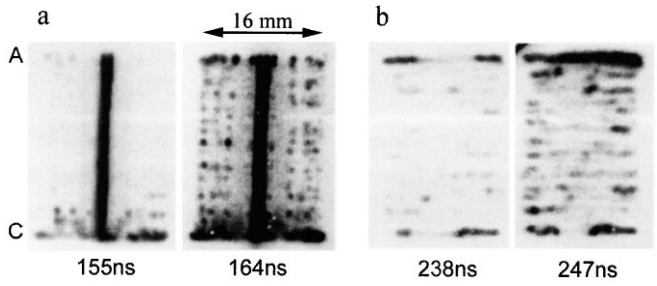

FIG. 4. Soft x-ray images showing formation of correlated bright spots due to the development of a global instability in arrays with 16 (a) and 64 (b) wires. Precursor plasma observed on the axis of 16 wire array is not seen with 64 wires.

TABLE I. Times of correlated bright spot formation (t_b) and their axial spacing (λ) in arrays with different numbers of wires. γ and G are the calculated growth rates and the number of e foldings of the Rayleigh-Taylor instability.

N	$I_{\max}$ (MA)	t_{imp} (ns)	t_b (ns)	λ (mm)	$\gamma(t_b)^{-1}$ (ns)	$G = \int \gamma\, dt(t_b)$
8	1.0	200	166	1.8	10.7	5.6
16	1.4	200	171	1.7	9.7	6
32	1.4	230	202	1.8	8.2	6.7
64	1.4	260	245	2.3	12.3	7.1

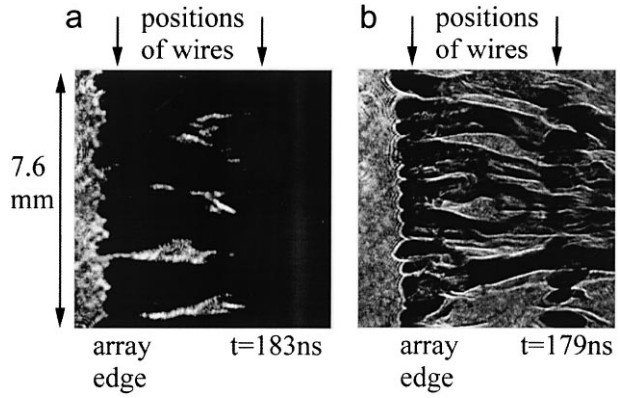

FIG. 5. Side-on laser schlieren (a) and shadow (b) images during the global instability development in 8 wire array.

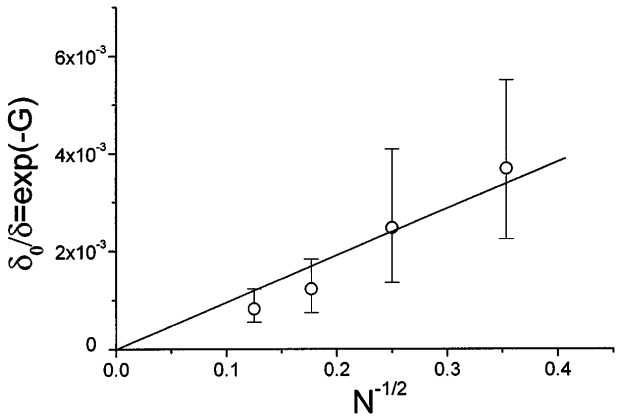

FIG. 6. Fit of the experimental data to the scaling law of Eq. (1). The error bars are due to uncertainty in the time of appearance of bright spots, equal to half of the x-ray camera interframe separation.

$\delta = \delta_0 \exp(G)$, where $G \equiv \int_0^t \gamma(t)\,dt$, $\gamma = \sqrt{g2\pi/\lambda}$, and g is the acceleration. A heuristic model by Haines [8] suggests a scaling for the seeded level of radial perturbations δ_0 with number of wires as $\delta_0 \propto N^{-1/2}$, due to averaging of the uncorrelated MHD instabilities which initially develop in individual wires. In this case, at the time when perturbations reach a fixed amplitude δ_*, the number of e foldings G will be related to the number of wires N, according to

$$\exp(-G) = \delta_0/\delta_* \propto N^{-1/2}. \tag{1}$$

For our experimental conditions the growth rate γ and the value of G at the time of the appearance of the bright spots in the x-ray images was calculated using the measured instability wavelengths $\lambda = 1.7$–2.3 mm and taking acceleration g from 0D calculations of the radius versus time (which agrees with experimental streak photographs for large numbers of wires). At the moment of bright spot observation, the calculated γ^{-1} of between 8.2 and 12.3 ns (see Table I) for different numbers of wires agrees with the observed fast formation of the spots in about the interframe time of the x-ray camera (9 ns). The calculated value of G increases with the number of wires from 5.6 to 7.1, and the plot in Fig. 6 shows that the experimental data agree reasonably well with the above scaling law. However, the possibility of another interpretation of the observed scaling cannot be excluded.

In conclusion, we have measured the spatial and temporal variation of plasma parameters in wire array z pinches with 8–64 wires. Azimuthal structure of the plasma inside the array was measured for the first time by end-on laser probing. Early expansion of individual wires in the array occurs with the development of uncorrelated MHD instabilities, similar to single wire explosions. The plasma moves inward from the wires towards the array axis four times faster than in the azimuthal direction, due to the global magnetic field of the array. The coronal plasmas from adjacent wires with density of 10^{17} cm^{-3} merge in 65–90 ns, depending on the wire separation. During the implosion, the development of an $m = 0$ instability with a dominant wavelength of 1.7–2.3 mm was detected. The time when the instability reaches the observable level corresponds to the number of e foldings for the growth of the classical RT of $\int \gamma\,dt \sim 5.6$–7. Scaling of this number with the number of wires in the array is consistent with the hypothesis that the global instability grows from seeded perturbations due to the averaging of the uncorrelated instabilities in individual wires.

[1] N. R. Pereira and J. Davis, J. Appl. Phys. **64**, R1 (1988).
[2] M. K. Matzen, Phys. Plasmas **4**, 1519 (1997).
[3] R. B. Spielman *et al.,* Phys. Plasmas **5**, 2105 (1998).
[4] T. W. L. Sanford *et al.,* Phys. Plasmas **4**, 2188 (1997).
[5] D. L. Peterson *et al.,* Phys. Plasmas **3**, 368 (1996).
[6] I. K. Aivazov *et al.,* Sov. J. Plasma Phys. **14**, 110 (1988).
[7] C. Deeney *et al.,* Rev. Sci. Instrum. **68**, 653 (1997).
[8] M. G. Haines, IEEE Trans. Plasma Sci. **26**, 1275 (1998).
[9] I. H. Mitchell *et al.,* Rev. Sci. Instrum. **67**, 1533 (1996).
[10] J. P. Chittenden *et al.,* Phys. Plasmas **4**, 4309 (1997).
[11] D. Mosher and D. Colombant, Phys. Rev. Lett. **68**, 2600 (1992).
[12] D. Kalantar and D. Hammer, Phys. Rev. Lett. **71**, 3806 (1993).
[13] F. N. Beg *et al.,* Plasma Phys. Control. Fusion **39**, 1 (1997).
[14] C. Deeney *et al.,* Phys. Rev. E **51**, 4823 (1995).
[15] T. W. Hussey *et al.,* J. Appl. Phys. **51**, 1452 (1980).
[16] J. H. Hammer *et al.,* Phys. Plasmas **3**, 2063 (1996).
[17] J. S. De Groot *et al.,* Phys. Plasmas **4**, 737 (1997).
[18] C. Deeney *et al.,* Phys. Rev. E **56**, 5945 (1997).